

Additional services for **Journal of Materials Research**:

Email alerts: [Click here](#)

Subscriptions: [Click here](#)

Commercial reprints: [Click here](#)

Terms of use : [Click here](#)

## Hidden parameters in the plasma deposition of microcrystalline silicon solar cells

M.N. van den Donker, B. Rech, R. Schmitz, J. Klomfass, G. Dingemans, F. Finger, L. Houben, W.M.M. Kessels and M.C.M. van de Sanden

Journal of Materials Research / Volume 22 / Issue 07 / 2007, pp 1767 - 1774  
DOI: 10.1557/jmr.2007.0226

**Link to this article:** [http://journals.cambridge.org/abstract\\_S0884291400025309](http://journals.cambridge.org/abstract_S0884291400025309)

### How to cite this article:

M.N. van den Donker, B. Rech, R. Schmitz, J. Klomfass, G. Dingemans, F. Finger, L. Houben, W.M.M. Kessels and M.C.M. van de Sanden (2007). Hidden parameters in the plasma deposition of microcrystalline silicon solar cells. *Journal of Materials Research*, 22, pp 1767-1774 doi:10.1557/jmr.2007.0226

**Request Permissions :** [Click here](#)

# OUTSTANDING MEETING PAPERS

*Papers in this section are based on submissions to the MRS Symposium Proceedings that were selected by Symposium Organizers as the outstanding paper. Upon selection, authors are invited to submit their research results to Journal of Materials Research. These papers are subject to the same peer review and editorial standards as all other JMR papers. This is another way by which the Materials Research Society recognizes high quality papers presented at its meetings.*

## Hidden parameters in the plasma deposition of microcrystalline silicon solar cells

M.N. van den Donker,<sup>a)</sup> B. Rech,<sup>b)</sup> R. Schmitz, J. Klomfass, G. Dingemans, and F. Finger<sup>c)</sup>

*Institut für Energieforschung-Photovoltaik (IPV), Forschungszentrum Jülich GmbH, Jülich 52425, Germany*

L. Houben

*Institut für Festkörperforschung (IFF), Forschungszentrum Jülich GmbH, Jülich 52425, Germany*

W.M.M. Kessels and M.C.M. van de Sanden

*Applied Physics, Technical University (TU) Eindhoven, Eindhoven 5600MB, The Netherlands*

(Received 2 January 2007; accepted 21 March 2007)

The effect of process parameters on the plasma deposition of  $\mu$ c-Si:H solar cells is reviewed in this article. Several *in situ* diagnostics are presented, which can be used to study the process stability as an additional parameter in the deposition process. The diagnostics were used to investigate the stability of the substrate temperature during deposition at elevated power and the gas composition during deposition at decreased hydrogen dilution. Based on these investigations, an updated view on the role of the process parameters of plasma power, heater temperature, total gas flow rate, and hydrogen dilution is presented.

### I. INTRODUCTION

Microcrystalline silicon ( $\mu$ c-Si:H) provides a promising route toward solar cells with high stabilized efficiency and cost-effective large-area production.<sup>1,2</sup> Figure 1 shows a transmission electron microscope (TEM) image of a single-junction  $\mu$ c-Si:H solar cell, consisting of glass, textured ZnO,  $\mu$ c-Si:H *p-i-n* junction, and back contact. Deposition of the intrinsic  $\mu$ c-Si:H film takes place in vapor-phase vacuum processes involving a silicon-containing source gas. The deposition process has received considerable scientific interest since the deposited material quality and the deposition rate at which it is obtained are crucial to the performance and price of eventually produced commercial solar modules.

A commonly used source gas is SiH<sub>4</sub>. Reactive radicals are formed from this gas by (for example) thermal dissociation using a hot wire or electron-impact dissociation using plasma. Known plasma sources are, for example, an expanding thermal plasma,<sup>3</sup> inductively-coupled plasma,<sup>4</sup> or microwave plasma.<sup>5</sup> In this work, we restricted ourselves to the parallel plate plasma source. This specific plasma source is used commonly in research and industry. Thus far, it has shown to be the best solar cell performance at high rate. It consists of two parallel electrodes, of which one is grounded (the substrate) and the other provided with an oscillating voltage signal (the powered electrode). Source gases are fed into the space enclosed by the electrodes. When the plasma is ignited, a film is deposited on both the substrate and the powered electrode.

We first provide a comprehensive literature review on the role of the various process parameters in the deposition process (pressure, gas mixture, etc.). Next, we discuss recent experimental results on the stability of the deposition process and experimentally demonstrate how these plasma instabilities act as hidden parameters in the deposition process. We conclude with an updated view on the role of the various process parameters in the deposition process.

<sup>a)</sup>Present address: Solland Solar Cells BV, Bohr 10, 6422 RL, Heerlen, The Netherlands

<sup>b)</sup>Present address: Department Silicon Photovoltaics (SE1), Hahn-Meitner-Institut Berlin, Kekuléstraße 5, 12489 Berlin, Germany

<sup>c)</sup>Address all correspondence to this author.

e-mail: f.finger@fz-juelich.de

This paper was selected as the Outstanding Meeting Paper for the 2006 MRS Spring Meeting Symposium A Proceedings, Vol. 910. DOI: 10.1557/JMR.2007.0226

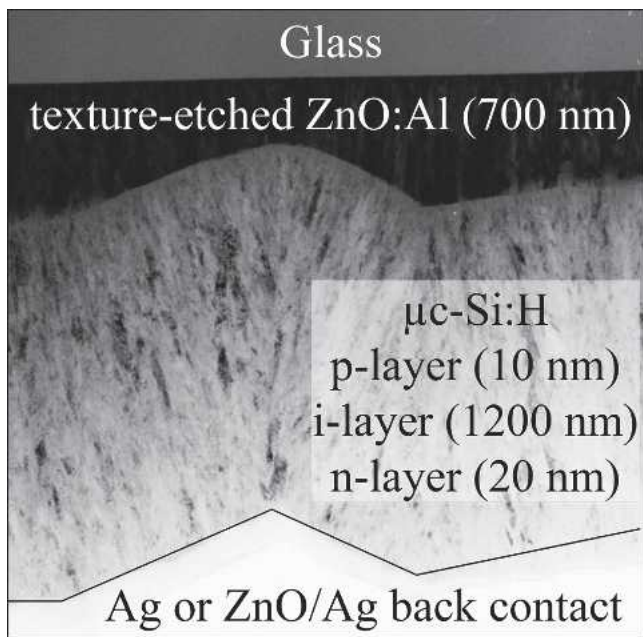


FIG. 1. TEM micrograph of a single-junction  $\mu$ c-Si:H solar cell. Glass coated with texture-etched ZnO:Al functions as substrate. The  $\mu$ c-Si:H *p-i-n* device is deposited on top of it. Typical thicknesses of the various layers are indicated in the figure.

## II. ROLE OF PROCESS PARAMETERS

The process parameters in the parallel plate plasma deposition technique are the plasma power  $P$ , gas pressure  $p$ , total gas flow rate  $Q$ , hydrogen dilution ratio  $R = H_2$  flow rate / SiH<sub>4</sub> flow rate [or alternatively silane concentration  $SC = SiH_4$  flow rate / (SiH<sub>4</sub> flow rate + H<sub>2</sub> flow rate)], temperature  $T$ , excitation frequency  $\omega$ , electrode area  $A$ , and electrode gap  $h$ . Previous studies exerted at the Institute of Photovoltaics, Jülich (IPV) led to a detailed picture on the role of the process parameters in the optimization of the deposition process of  $\mu$ c-Si:H toward higher deposition rates and better material quality. In the following we provide a review.

### A. $R$

The H<sub>2</sub> dilution ratio is obtained by dividing the H<sub>2</sub> flow rate into that of SiH<sub>4</sub>. It is considered to be one of the most important parameters for deposition of  $\mu$ c-Si:H. If the H<sub>2</sub> dilution ratio is changed, the material can be tuned from being purely amorphous to being highly crystalline.<sup>6</sup> Usually, the best solar cell performance is obtained using material with a crystalline volume fraction in the range of ~60–70%.<sup>6,7</sup> There is no “ideal” dilution ratio necessary for obtaining this transition-type material. For example, the best solar cells are obtained at a dilution ratio of ~20 using very high frequency (VHF) deposition at low pressure,<sup>6</sup> ~10 using VHF deposition at high pressure,<sup>8</sup> and ~150 using radio frequency (rf) deposition at high pressure.<sup>9</sup>

### B. $P$

The power coupled into the plasma mainly influences the deposition rate. The power does not influence deposition rate directly under conditions of high SiH<sub>4</sub> depletion.<sup>8,9</sup> Instead, under these conditions, the power influences the dilution ratio for which  $\mu$ c-Si:H with optimized crystalline volume fraction can be obtained. In other words, for high plasma power, one can use a low dilution ratio and therefore deposit at high rate. Unfortunately, the power also influences the material quality. The material quality, for example expressed in terms of the solar cell performance, steadily deteriorates as the plasma power is increased. The optimum regarding high deposition rate at state-of-the-art material quality was on the order of 10<sup>2</sup> W for a 10 × 10 cm<sup>2</sup> substrate size reactor in Refs. 8 and 9.

### C. $p$

The deposition pressure mainly influences the material quality, in that it may compensate for the damaging effect of a high power. This effect of the pressure was investigated in detail in Ref. 9 for rf deposition. For each pressure, the plasma power and dilution ratio were adjusted to obtain material of the same deposition rate and the same crystalline volume fraction. A clear “threshold” pressure was seen, above which the device performance was good. The dependence of this “threshold” pressure on other process parameters requires further investigation. Deposition at elevated pressure ( $p \geq 1$  Torr) is generally referred to as the “high pressure depletion regime” and was used, for example, in Refs. 1, 2, 8–10.

### D. $Q$

The best solar cell performance is usually found at the highest possible total flow rate [in a 10 × 10 cm<sup>2</sup> substrate size reactor up to 400 sccm (standard cm<sup>3</sup> per min) was investigated for VHF deposition in Ref. 8 and flow rates of up to 1000 sccm for rf deposition in Ref. 11]. On the other hand, source gas utilization was found to improve for low total flow rate in Ref. 11. The optimum for total gas flow rate regarding efficient gas usage and state-of-the-art material quality was on the order of 10<sup>2</sup> sccm in Refs. 8 and 11.

### E. $\omega$

The optimum substrate temperature was determined to be ~200 °C for rf deposition at high pressure in Ref. 12. This value did not depend on the pressure. Other dependencies are yet to be investigated.

### F. $\omega$

The conventional excitation frequency used by industry is 13.56 MHz (commonly referred to as rf deposition).

At higher excitation frequencies (up to  $\sim$ 100 MHz, commonly referred to as VHF deposition) a higher deposition rate without any deterioration in the quality of the material has been obtained.<sup>8</sup> However, for high excitation frequency, effects such as standing-waves lead to poor homogeneity.<sup>13</sup> The optimum for excitation frequency regarding high deposition rate, state-of-the-art material quality, and sufficient homogeneity is yet to be determined.

### G. A

To realize cost-effective production, the deposition processes eventually have to be scaled-up to electrode areas of square meters and beyond. References 2 and 9 deal with this issue of up-scaling. The total gas flow rate has to be increased to a larger electrode area. Standing waves may influence voltage uniformity at large electrode area. These effects are still under investigation.

### H. h

State-of-the-art material quality at high rate was found for an electrode gap of 1.0 cm using rf deposition at high pressure.<sup>9</sup> This ideal electrode gap may depend on pressure and power. Namely, the power necessary for plasma ignition depends strongly on the product of pressure and electrode gap.<sup>14</sup> The investigation on the minimum power needed for plasma ignition from Ref. 8 illustrates this. It is an engineering challenge to realize a small electrode gap with low tolerance in a large area deposition setup. The optimum electrode gap regarding homogeneity may therefore also depend on the used electrode area.

## III. ROLE OF HIDDEN PARAMETERS

The review above indicates that every single process parameter plays a distinct role in the deposition process. Because the best material is found close to the transition to a-Si:H, the process window for obtaining state-of-the-art material quality is small with respect to each process parameter. Figure 2 illustrates this by showing a typical  $\mu$ c-Si:H single junction solar cell deposition series in which the deposition pressure was varied around the optimum conditions in the high pressure depletion regime. In these conditions, the process window for the pressure was located between 10 and 12 Torr. The narrow process window sets high demands on the process stability. A drift of  $\sim$ 10% may already induce the transition to a-Si:H growth. Thus, the process stability can be regarded as an extra parameter that influences the material properties in addition to the parameters described above. This parameter remains “hidden” unless it is uncovered using in situ process diagnostics.

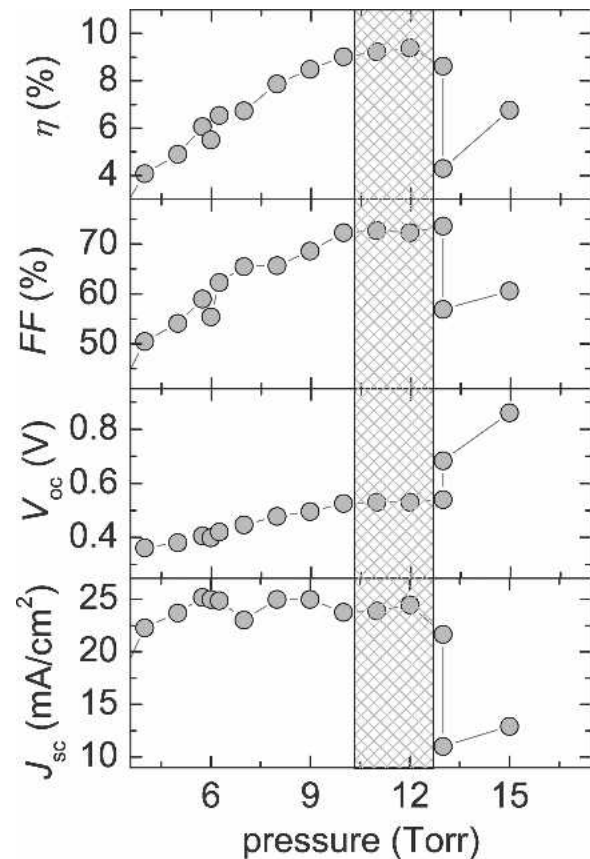


FIG. 2. Solar cell parameters—efficiency  $\eta$ , fill-factor  $FF$ , open-circuit voltage  $V_{oc}$ , and short-circuit current  $J_{sc}$ —as a function of a variation of the deposition pressure at otherwise constant process parameters. The marked area indicates the small process window for preparation of optimum quality material.

### A. Experimental details

Experiments on the process stability were performed in a multichamber vacuum system consisting of five deposition chambers and three load and transfer chambers. The chamber used for intrinsic  $\mu$ c-Si:H deposition consisted of two parallel electrodes of which the upper electrode was grounded and could be mounted with  $10 \times 10 \text{ cm}^2$  sized substrate. The lower, cylindrical electrode of  $150 \text{ cm}^2$  area was powered by a 13.56 MHz rf generator. The  $\text{H}_2 + \text{SiH}_4$  source gas was supplied through showerhead holes in this electrode. An Oriel MS257 spectrometer was used to record the time-resolved optical emission spectroscopy (OES). We measured intensities of the atomic lines  $\text{H}_\alpha$  (3–2 at 656 nm),  $\text{H}_\beta$  (4–2 at 486 nm), Si ( $4s^1\text{P}^0 - 3p^2\text{1S}$  at 390 nm), and of the molecular bands of  $\text{H}_2$  ( $3p^3\Pi_u^- - 2s^3\Sigma_g^+$  around 602 nm) and  $\text{SiH}$  ( $A^2\Delta - X^2\Pi$  around 414 nm). An Impac IN 5/5 pyrometer was used to monitor the substrate temperature. The substrate was monitored from behind to avoid influences of the plasma and depositing film on the surface emissivity.

We used several sets of deposition conditions. The

standard conditions, obtained in successive optimization steps described in Refs. 9, 11, and 12, are defined by  $\{R, P, p, Q, T, h, \omega, A, h_w\} = \{150, 60 \text{ W}, 10 \text{ Torr}, 500 \text{ sccm}, 200^\circ\text{C}, 13.56 \text{ MHz}, 150 \text{ cm}^2, 1.0 \text{ cm}\}$ . Single-junction  $\mu\text{c-Si:H}$  solar cells were prepared using texture-etched  $\text{ZnO:Al}$  on glass as substrate.<sup>2,15,16</sup> The  $p$ - and  $n$ -type doped layers were deposited in separate chambers by using an admixture of  $\text{B}(\text{CH}_3)_3$  (trimethylborane, TMB) and  $\text{PH}_3$  (phosphine) gas, respectively. Sputtered  $\text{ZnO}$  and evaporated  $\text{Ag}$  served as the back contact and defined the solar cell area of  $1 \text{ cm}^2$ . The solar cell performance was characterized by air mass (AM) 1.5 illuminated current–voltage measurements at  $25^\circ\text{C}$  using a class A double-source solar simulator. Raman spectroscopy using 488-nm laser excitation was performed on some selected solar cells after etching off the  $n$ -layer with potassium hydroxide. The Raman intensity ratio, determined from a division of the crystalline to the total contribution of the Raman scattered light, served as an estimation of the crystalline volume fraction.<sup>7</sup>

## B. Hidden parameter in the plasma power

This study was performed using the standard conditions of rf deposition for which the plasma power, substrate temperature, and  $\text{SiH}_4$  flow rate were varied. The first results were published in Ref. 17. Plasma powers of 60, 80, and 200 W were investigated. At each plasma power, a series of solar cells was deposited at varying substrate temperature and  $\text{SiH}_4$  flow rate. The best cells from these series are plotted in Fig. 3. The figure shows that a high plasma power was essential for obtaining a high deposition rate. To obtain the maximum solar cell performance at the high plasma power, the heater temperature had to be set to a lower value. Unfortunately, even for this adapted heater power, the solar cell performance still steadily decreased for increasing plasma power. Note that the solar cell data are in good agreement with a more extensive study carried out on the same reactor in previous work.<sup>9</sup>

The decreasing optimized heater temperature for increasing plasma power can be understood from the heat load of the plasma. The plasma power is used to overcome potential barriers in the transformation of  $\text{SiH}_4$  molecules to the  $\mu\text{c-Si:H}$  film. However, in the end, essentially all plasma power will be converted to heat, which has to leave the system via the walls and electrodes. Thus, to stay within the process window for the substrate temperature around  $200^\circ\text{C}$ , the heater temperature has to be decreased if the plasma power is increased. Because the plasma power is abruptly switched on when deposition starts, an increasing temperature profile is expected to develop during deposition.

By *in situ* substrate temperature measurements using the pyrometer, we indeed experimentally found the substrate temperature to increase by  $80^\circ\text{C}$  during deposition

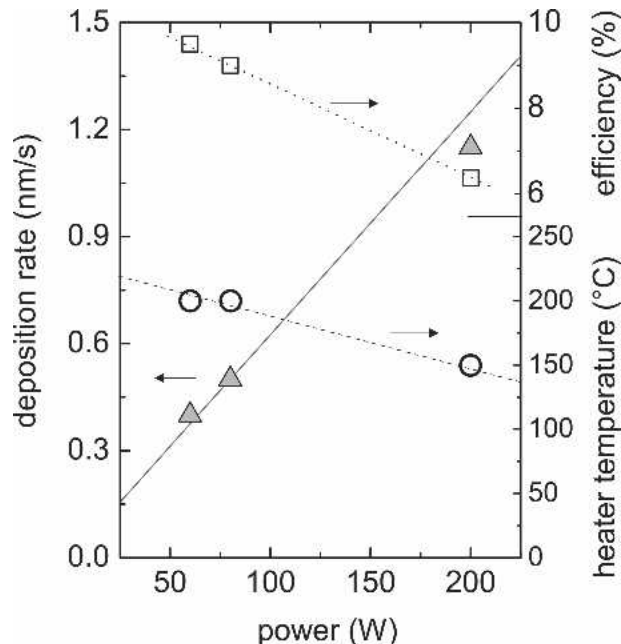


FIG. 3. Deposition rate (solid triangles, solid line as guide to the eye), heater temperature (open circles, dashed line as guide to the eye), and solar cell efficiency (open squares, dotted line as guide to the eye) obtained as a function of the applied plasma power. Figure is partly based on data from Ref. 17.

at 200 W, as illustrated in Fig. 4. Plasma-induced substrate heating was thus found to be an important hidden parameter. It was made visible using an *in situ* diagnostic for detecting the time-dependent substrate temperature.

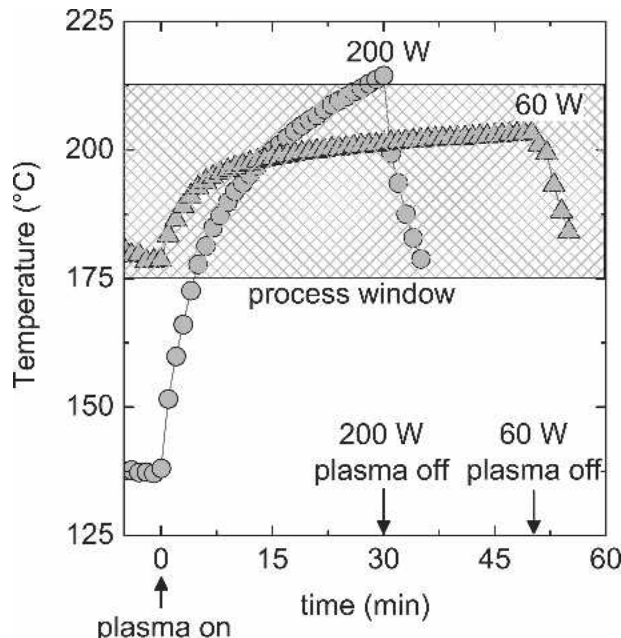


FIG. 4. Substrate temperature measured *in situ* during deposition of an optimized  $\mu\text{c-Si:H}$  film at 60 W (solid triangles) and 200 W (solid circles). The marked area indicates the process window for obtaining optimum quality material. Figure is partly based on data from Ref. 17.

We managed to prevent this substrate temperature increase for deposition at 80 W by gradually decreasing the heater temperature during deposition. For a plasma power of 200 W, this procedure was insufficient; even when the heater was completely switched off after plasma ignition, the substrate temperature still increased during deposition. Thus, for high-rate deposition, an active substrate temperature control with a fast response time has to be developed and installed.

### C. Hidden parameter in the hydrogen dilution

This study was performed using the mentioned standard conditions of rf deposition for which the total flow rate and dilution ratio were varied. The first results were published in Ref. 18. Several conditions of total flow rate were investigated, varying from a high total flow rate of 1000 sccm to a small total flow rate of only 2 sccm.

Figure 5 shows a comparison of solar cell efficiency, dilution ratio, and source gas utilization. At each  $H_2$  flow rate, a solar cell deposition series was carried out as a function of the  $SiH_4$  flow rate. The properties of best cells obtained in each of these deposition series are plotted as a function of the corresponding  $H_2$  flow rate. The source gas utilization was derived from the ratio of deposition rate to  $SiH_4$  flow rate, according to

$$\eta_{gas} = 2 An_{\mu c} r_d / S_{feed} \quad (1)$$

where  $\eta_{gas}$  is the gas utilization efficiency,  $A$  is the electrode area,  $n_{\mu c}$  is the number density of silicon in  $\mu c-Si:H$ ,  $r_d$  is the deposition rate, and  $S_{feed}$  is the feed gas flow rate of  $SiH_4$  expressed in particles  $s^{-1}$ .

Figure 5 shows that deposition at low  $H_2$  flow rate requires a lower dilution ratio than deposition at high  $H_2$  flow rate. The advantage of deposition at low  $H_2$  gas

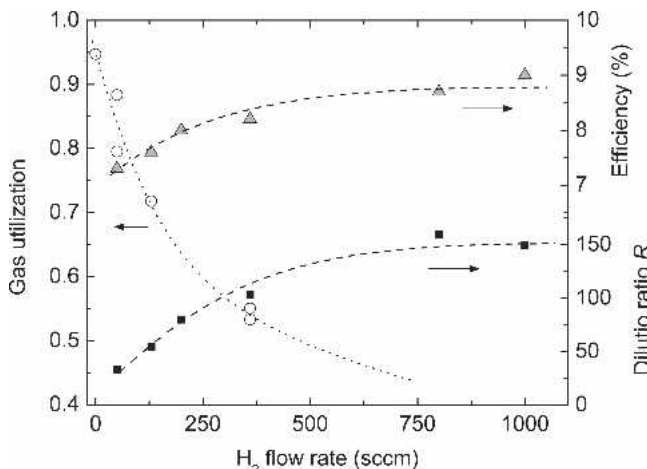


FIG. 5. Obtained solar cell efficiency (triangles) versus used  $H_2$  flow rate, together with the dilution ratio and the source gas utilization at which this efficiency was obtained (solid squares). The solar cell data were taken from Ref. 11.

flow rate is a high  $SiH_4$  gas utilization. In other words, for low  $H_2$  flow rate, the plasma efficiently converts  $SiH_4$  into  $H_2$  (and into the  $\mu c-Si:H$  film), thereby decreasing the need for additional  $H_2$  admixture in the feed gas flow. Unfortunately, even when the lowered dilution ratio is used, the obtained solar cell efficiency is lower for deposition at low  $H_2$  flow rate than that for deposition at a high  $H_2$  flow rate.

The primary cause for the low solar cell efficiency obtained in a low total gas flow regime is revealed by time resolved optical emission spectroscopy measurements. Figure 6 shows the  $SiH$  and  $Si$  emission intensity versus time after plasma ignition for four  $\{R, Q\}$  (sccm)-settings. Because of the higher intensity, the  $SiH$  emission has a better signal-to-noise ratio than the  $Si$  emission. One can see a clear trend going from a condition of high dilution ratio and high total flow rate toward a condition with low dilution ratio and low total flow rate. An initial enhancement and subsequent drop of the  $SiH$  and  $Si$  emission become more and more pronounced. This instability is ascribed to the decrease in gas-phase  $SiH_4$  as it becomes transiently depleted in the course of film growth<sup>18</sup> and interferes with successful nucleation of the  $\mu c-Si:H$  film. Transient  $SiH_4$  depletion was thus found to be an important hidden parameter. It was made visible using an in situ diagnostic for detecting the time-dependent gas composition.

In our previous work,<sup>18</sup> we developed a procedure to prevent the transient  $SiH_4$  depletion. In this procedure of tailored initial  $SiH_4$  density, we first fill the reactor with 10 Torr pure  $H_2$ . Then we close all gas valves. In a precisely timed order, we first switch on the process flow with the chosen  $\{R, Q\}$ -setting, and shortly afterwards ignite the plasma. When this procedure is applied, almost pure  $H_2$  is present in the reactor upon plasma ignition

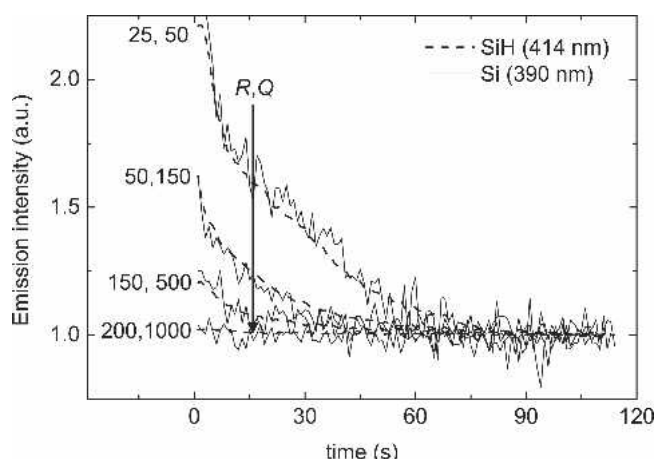


FIG. 6. Time-resolved optical emission intensity of the  $SiH$  emission at 414 nm and the  $Si$  emission at 390 nm for four different conditions of  $\{R, Q\}$  (sccm), namely  $\{25, 50\}$ ,  $\{50, 150\}$ ,  $\{150, 500\}$ , and  $\{200, 1000\}$ .

whereas a  $\text{SiH}_4 + \text{H}_2$  gas mixture enters through the gas supply line. This procedure allows for a comparison of high and low total flow rate deposition regimes to be made without the transient depletion instability influencing the experiment.

In the following measurements, we compare the highly  $\text{H}_2$  diluted regime of  $\{R = 150, Q = 500 \text{ sccm}\}$  with the pure  $\text{SiH}_4$  deposition condition of  $\{R = 0, Q = 2 \text{ sccm}\}$ . In the latter regime, the ignition procedure as described above was used to cancel out the influence of the transient depletion instability. Using optical emission spectroscopy, we qualitatively compare the gas composition of both regimes in Fig. 7. The spectra show similar features. In both cases, the major contribution to the integrated intensity originated from excited  $\text{H}_2$ , the most intense line was  $\text{H}_\alpha$ , and the relative contribution of  $\text{SiH}$  was small. The interpretation is that in the pure  $\text{SiH}_4$  regime, almost all  $\text{SiH}_4$  is depleted in deposition reactions, causing the gas composition to consist predominantly of  $\text{H}_2$  despite the fact that the feed gas flow consists solely of  $\text{SiH}_4$ . Figure 8 shows a comparison between the Raman spectra of films deposited in the two regimes. One can see that the Raman intensity ratio of the films is similar. For both the highly diluted and pure  $\text{SiH}_4$  deposition regimes the Raman crystallinity ratio equals the optimum value of  $\sim 60\text{--}70\%$ , which makes the material suitable for application in single-junction  $\mu\text{-Si:H}$  solar cells.

We prepared several solar cells in the highly  $\text{H}_2$  diluted regime and in the pure  $\text{SiH}_4$  deposition regime to demonstrate that both regimes are indeed capable of depositing material of good quality. Using the highly  $\text{H}_2$

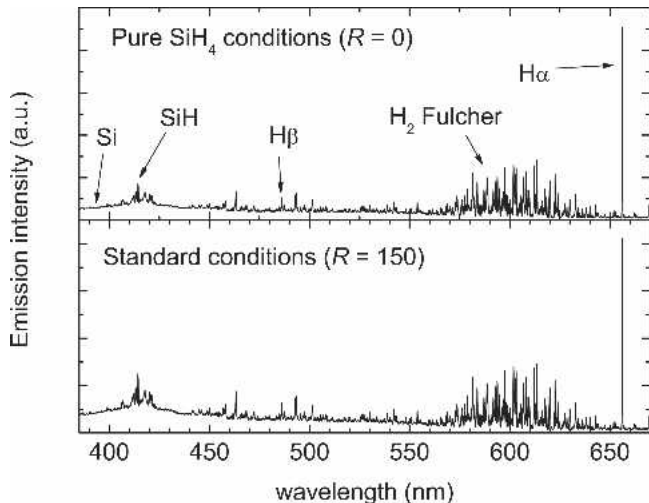


FIG. 7. Recorded optical emission spectrum for a plasma operated at the standard conditions of  $R = 150$  and  $Q = 500 \text{ sccm}$  and for a plasma operated at the pure  $\text{SiH}_4$  conditions of  $R = 0$  and  $Q = 2 \text{ sccm}$  (upper figure). In the upper figure, the relevant spectral parts for detection of  $\text{H}_\alpha$ ,  $\text{H}_\beta$ ,  $\text{H}_2$ ,  $\text{SiH}$ , and  $\text{Si}$  are indicated. The spectrum was not corrected for spectral sensitivity of the optical system.

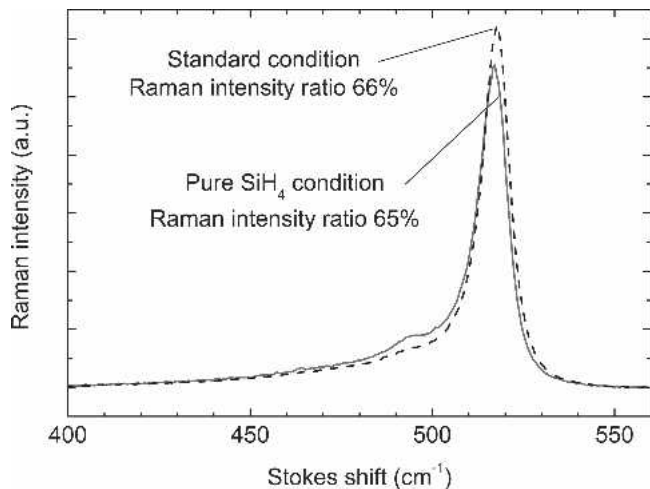


FIG. 8. Raman spectrum of a  $1\text{-}\mu\text{m}$ -thick film grown in the standard condition and in the pure  $\text{SiH}_4$  flow condition. For the pure  $\text{SiH}_4$  flow condition, the reactor was filled with  $\text{H}_2$  prior to plasma ignition to prevent the influence of transient depletion.

diluted regime (Fig. 5), we obtained a best-cell of  $1 \times 1 \text{ cm}^2$  with the current–voltage characteristic parameters under AM 1.5 illumination of efficiency  $\eta = 9.4\%$ , fill factor  $FF = 72\%$ , open-circuit voltage  $V_{\text{oc}} = 0.53 \text{ V}$ , and short-circuit current  $J_{\text{sc}} = 24 \text{ mA/cm}^2$  at a deposition rate of  $0.5 \text{ nm s}^{-1}$ . Using the pure  $\text{SiH}_4$  deposition regime,<sup>18</sup> we obtained the characteristic values of efficiency  $\eta = 9.5\%$ , fill factor  $FF = 75\%$ , open-circuit voltage  $V_{\text{oc}} = 0.56 \text{ V}$ , and short-circuit current  $J_{\text{sc}} = 22 \text{ mA/cm}^2$  at a deposition rate of  $0.4 \text{ nm s}^{-1}$ .

Apparently, for a given optimized  $\mu\text{-Si:H}$  deposition process in the rf high-pressure depletion regime, one can simply switch off the  $\text{H}_2$  flow, make a minor adjustment of the  $\text{SiH}_4$  flow rate, and end up with the same plasma and the same deposited material. The mere fact that one can prepare  $\mu\text{-Si:H}$  solar cells from pure  $\text{SiH}_4$  has been reported before, e.g., by Feitknecht et al.,<sup>19</sup> Roschek et al.,<sup>11</sup> and Strahm et al.<sup>20</sup> However, as we have demonstrated, controlling the process stability in this regime is of crucial importance. Namely, the initial phase of deposition is highly unstable and not well-defined under conditions of low flow rate and low  $\text{H}_2$  dilution, as Fig. 6 demonstrates. At average deposition rates of  $0.5 \text{ nm/s}$ , this 90 s initial phase corresponds to  $45 \text{ nm}$  of initial film with uncontrolled properties, which severely hampers the nucleation of the  $\mu\text{-Si:H}$  film and leads to poor material quality and solar cell efficiency. Until this instability was made visible and controlled, the pure  $\text{SiH}_4$  deposition regime was not accessible.

#### IV. UPDATED VIEW ON ROLE OF PROCESS PARAMETERS

Now that we understand and can control the hidden parameters of plasma-induced substrate heating and transient depletion, the view on the role of the power  $P$ ,

temperature  $T$ , total gas flow rate  $Q$ , and dilution ratio  $R$  needs to be updated.

### A. $P$

One of the reasons why the material quality and solar cell performance deteriorate for high-rate deposition is the fact that the high rf power needed for obtaining high rate leads to an increase in temperature during deposition via plasma-induced substrate heating.

### B. $T$

Under high-rate deposition conditions, the ideal substrate temperature of 200 °C cannot be maintained by a simple substrate temperature control that relies on the heat conductivity through the process gas mixture between a resistive heater mounted at some distance from the substrate in the reactor. Instead, heater temperature profiling or active cooling of the substrate becomes necessary.

### C. $Q$

In our investigation, state-of-the-art solar cell performance was obtained at an extremely low total flow rate of only 2 sccm. We conclude that under our conditions, the total flow rate does not have any effect on the deposition regime regarding material quality and deposition rate. In contrast, in Refs. 8 and 11, the best solar cell performance was found at maximized total flow rate. We thus speculate that the increasing solar cell performance with total flow rate found in these reports was in fact caused by the transient SiH<sub>4</sub> depletion becoming less pronounced at high total flow rate.

### D. $R$

The dilution ratio  $R$  has meaning only if viewed together with the SiH<sub>4</sub> depletion. We can distinguish between a regime of negligible SiH<sub>4</sub> depletion and a regime of significant SiH<sub>4</sub> depletion. In the first regime, the dilution ratio would be a useful quantity to describe the SiH<sub>4</sub> density in the plasma and characterize the deposition condition. Note that this regime is inefficient regarding source gas utilization and deposition rate and therefore has little technological relevance. In the second regime, which is of technological relevance, a change of H<sub>2</sub> flow rate hardly influences the partial H<sub>2</sub> and SiH<sub>4</sub> density. This places doubts on the capability of the dilution ratio to successfully characterize the deposition regime.

A useful quantity to characterize a regime of high depletion would be the SiH<sub>4</sub> flow rate scaled to the substrate size to be able to compare different reactor sizes. We can retrospectively apply this quantity of SiH<sub>4</sub> flow rate density to characterize deposition conditions from literature. For example, the rf deposition presented in this

study gives transition material at 0.5 nm/s for an SiH<sub>4</sub> flow rate density of ~0.02–0.04 sccm cm<sup>-2</sup> (at  $R$  between 0 and 150). The VHF deposition condition of Mai et al.<sup>8</sup> gives 0.6 nm/s transition material at an SiH<sub>4</sub> flow rate density of 0.04 sccm cm<sup>-2</sup> (at  $R$  equal to 20). We can also apply it to different deposition methods. For example, the expanding thermal plasma deposition from Ref. 3 yields transition material at 0.5 nm/s for a SiH<sub>4</sub> flow rate density of 0.02 sccm cm<sup>-2</sup> (at  $R$  equal to 300). The SiH<sub>4</sub> flow rate density was in the range 0.02–0.04 sccm cm<sup>-2</sup> for all these examples from literature.

## V. CONCLUSIONS

Because of the small process window for obtaining state-of-the-art solar cell performance, the stability of the microcrystalline silicon deposition process is an important hidden parameter, significantly influencing the material and solar cell properties. We explored the process stability of the high pressure depletion deposition regime using *in situ* diagnostics. Under conditions of elevated plasma power, the substrate temperature becomes unstable due to the heat load of the plasma. Under conditions of low total flow rate and low dilution ratio, the gas composition becomes unstable due to the transient depletion of the initially present SiH<sub>4</sub> source gas. By actively controlling the substrate temperature and gas composition, these deposition regimes of high plasma power and low total flow rate—yielding high deposition rates and effective gas utilization, respectively—should become accessible for deposition of state-of-the-art microcrystalline silicon solar cells.

## ACKNOWLEDGMENTS

The authors kindly thank W. Appenzeller, F. Birmans, R. Carius, A. Gordijn, M. Hülsbeck, D. Grunsky, Y. Mai, and S. Reynolds for fruitful discussions and experimental support. Helianthos BV is acknowledged for financial support. The research of W.M.M. Kessels was made possible through a fellowship of the Royal Netherlands Academy of Arts and Sciences (KNAW).

## REFERENCES

1. K. Yamamoto, M. Yoshimi, Y. Tawada, S. Fukuda, T. Sawada, T. Meguro, H. Takata, T. Suezaki, Y. Koi, K. Hayashi, T. Suzuki, M. Ichikawa, and A. Nakajima: Large area thin film Si module. *Sol. Energy Mater. Sol. Cells* **74**, 449 (2002).
2. B. Rech, T. Repmann, M.N. van den Donker, M. Berginski, T. Kilper, J. Hüpkens, S. Calnan, H. Stiebig, and S. Wieder: Challenges in microcrystalline silicon based solar cell technology. *Thin Solid Films* **511–512**, 548 (2006).
3. C. Smit, E.A.G. Hamers, B.A. Korevaar, R.A.C.M.M. van Swaaij, and M.C.M. van de Sanden: Fast deposition of microcrystalline

silicon with an expanding thermal plasma. *J. Non-Cryst. Solids* **299–302**, 98 (2002).

4. N. Kosku, F. Kurisu, M. Takegoshi, H. Takahashi, and S. Miyazaki: High-rate deposition of highly crystallized silicon films from inductively coupled plasma. *Thin Solid Films* **435**, 39 (2003).
5. H. Shirai, T. Arai, and H. Ueyama: The generation of high-density microwave plasma and its application to large-area microcrystalline silicon thin film formation. *Jpn. J. Appl. Phys.* **37**, L1078 (1998).
6. O. Vetterl, F. Finger, R. Carius, P. Hapke, L. Houben, O. Kluth, A. Lambertz, A. Mück, B. Rech, and H. Wagner: Intrinsic microcrystalline silicon: A new material for photovoltaics. *Sol. Energy Mater. Sol. Cells* **62**, 97 (2000).
7. L. Houben, M. Luysberg, P. Hapke, R. Carius, F. Finger, and H. Wagner: Structural properties of microcrystalline silicon in the transition from highly crystalline to amorphous growth. *Philos. Mag. A* **77**, 1447 (1998).
8. Y. Mai, S. Klein, R. Carius, J. Wolff, A. Lambertz, F. Finger, and X. Geng: Microcrystalline silicon solar cells deposited at high rates. *J. Appl. Phys.* **97**, 114913 (2005).
9. B. Rech, T. Roschek, T. Repmann, J. Müller, R. Schmitz, and W. Appenzeller: Microcrystalline silicon for large area thin film solar cells. *Thin Solid Films* **427**, 157 (2003).
10. M. Kondo, M. Fukawa, L. Guo, and A. Matsuda: High rate growth of microcrystalline silicon at low temperatures. *J. Non-Cryst. Solids* **266–269**, 84 (2000).
11. T. Roschek, B. Rech, J. Müller, R. Schmitz, and H. Wagner: Influence of the total gas flow on the deposition of microcrystalline silicon solar cells. *Thin Solid Films* **451–452**, 466 (2004).
12. T. Roschek, T. Repmann, J. Müller, B. Rech, and H. Wagner: Comprehensive study of microcrystalline silicon solar cells deposited at high rate using 13.56 MHz plasma-enhanced chemical vapor deposition. *J. Vac. Sci. Technol. A* **20**, 492 (2002).
13. L. Sansonnens, A. Pletzer, D. Magni, A.A. Howling, Ch. Hollenstein, and J.P.M. Schmitt: A voltage uniformity study in large-area reactors for RF plasma deposition. *Plasma Sources Sci. Technol.* **6**, 170 (1997).
14. V.A. Lisovskiy and V.D. Yegorenkov: Rf breakdown of low-pressure gas and a novel method for determination of electron-drift velocities in gases. *J. Phys. D Appl. Phys.* **31**, 3349 (1998).
15. O. Kluth, B. Rech, L. Houben, S. Wieder, G. Schöpe, C. Beneking, H. Wagner, A. Löfli, and H.W. Schock: Texture etched ZnO:Al coated glass substrates for silicon based thin film solar cells. *Thin Solid Films* **351**, 247 (1999).
16. O. Kluth, G. Schöpe, J. Hüpkens, C. Agashe, J. Müller, and B. Rech: Modified Thornton model for magnetron sputtered zinc oxide: Film structure and etching behaviour. *Thin Solid Films* **442**, 80 (2003).
17. M.N. van den Donker, R. Schmitz, W. Appenzeller, B. Rech, W.M.M. Kessels, and M.C.M. van de Sanden: The role of plasma induced substrate heating during high-rate deposition of microcrystalline silicon solar cells. *Thin Solid Films* **511–512**, 562 (2006).
18. M.N. van den Donker, B. Rech, F. Finger, W.M.M. Kessels, and M.C.M. van de Sanden: Highly efficient microcrystalline silicon solar cells deposited from a pure SiH<sub>4</sub> flow. *Appl. Phys. Lett.* **87**, 263503 (2005).
19. L. Feitknecht, J. Meier, P. Torres, J. Zürcher, and A. Shah: Plasma deposition of thin film silicon: Kinetics monitored by optical emission spectroscopy. *Sol. Energy Mater. Sol. Cells* **74**, 539 (2002).
20. B. Strahm, A.A. Howling, L. Sansonnens, Ch. Hollenstein, U. Kroll, J. Meier, Ch. Ellert, L. Feitknecht, and C. Ballif: Microcrystalline silicon deposited at high rate on large areas from pure silane with efficient gas utilization. *Sol. Energy Mater. Sol. Cells* **91**, 495 (2007).